

# **Gold nanoaggregates for probing single-living cell based on surface- enhanced Raman spectroscopy**

Peng Lu  
Jing Wang  
Jinyong Lin  
Juqiang Lin  
Nenrong Liu  
Zufang Huang  
Buhong Li  
Haishan Zeng  
Rong Chen

# Gold nanoaggregates for probing single-living cell based on surface-enhanced Raman spectroscopy

Peng Lu,<sup>a,†</sup> Jing Wang,<sup>a,†</sup> Jinyong Lin,<sup>a,†</sup> Juqiang Lin,<sup>a,\*</sup> Nenrong Liu,<sup>a</sup> Zufang Huang,<sup>a</sup> Buhong Li,<sup>a</sup> Haishan Zeng,<sup>b</sup> and Rong Chen<sup>a,\*</sup>

<sup>a</sup>Fujian Normal University, Ministry of Education and Fujian Provincial Key Laboratory for Photonics Technology, Key Laboratory of Optoelectronic Science and Technology for Medicine, Fuzhou 350007, China

<sup>b</sup>British Columbia Cancer Research Centre, Imaging Unit-Integrative Oncology Department, Vancouver, British Columbia, V5Z 1L3 Canada

**Abstract.** Gold nanoparticles are delivered into living cells by transient electroporation method to obtain intracellular surface-enhanced Raman spectroscopy (SERS). The subcellular localization of gold nanoparticles is characterized by transmission electron microscopy, and the forming large gold nanoaggregates are mostly found in the cytoplasm. The SERS detection of cells indicates that this kind of gold nanostructures induces a high signal enhancement of cellular chemical compositions, in addition to less cellular toxicity than that of silver nanoparticles. These results demonstrate that rapid incorporation of gold nanoparticles by electroporation into cells has great potential applications in the studies of cell biology and biomedicine. © 2015 Society of Photo-Optical Instrumentation Engineers (SPIE) [DOI: 10.1117/1.JBO.20.5.051005]

Keywords: gold nanoparticles; surface-enhanced Raman spectroscopy; electroporation; cell analysis.

Paper 140419SSPR received Jun. 30, 2014; accepted for publication Oct. 21, 2014; published online Nov. 11, 2014.

## 1 Introduction

Raman spectroscopy, which provides molecular and structural information of biological samples, is playing an increasingly vital role in biomedical analysis in recent years. In particular, because of its narrow Raman bands and low water influence, Raman spectroscopy is suitable for characterizing the compositions of complex biochemical mixtures.<sup>1</sup> Raman scattering is an extremely weak effect since the typical Raman cross section is between  $10^{-31}$  and  $10^{-29}$  cm<sup>2</sup> per molecule.<sup>2</sup> However, with the emergence of surface-enhanced Raman scattering (SERS) spectroscopy, Raman signals can be enhanced by many orders of magnitude ( $10^2$  to  $10^{14}$  times).<sup>3,4</sup>

“Passive uptake” is one of the most common methods used for delivering silver or gold nanoparticles into cells.<sup>5–7</sup> However, this approach is time-consuming in that cells need to be incubated with nanoparticles for several hours or even more, and the amount of nanoparticles delivered into the cells is highly dependent upon the physical dimension of the nanoparticles.<sup>8</sup> To address these issues, we have successfully delivered silver nanoparticles into the cells through electroporation, which is much faster and more efficient than the “passive uptake” method.<sup>9</sup> Notably, however, gold nanoparticles are preferred over silver nanoparticles in many biomedical applications because of their favorable physical and chemical properties and biocompatibility.<sup>10,11</sup> Near-infrared (NIR) is also the desired excitation range for Raman detection of cells because the lower-energy photons reduce the fluorescence background in biological samples and decrease the risk of cell degeneration.<sup>11,12</sup> Meanwhile, gold nanoparticles have comparably good SERS enhancement factors as silver nanoparticles when NIR excitation is applied.<sup>12</sup> In this study, we explore the use of gold nanoparticles and NIR laser excitation for SERS application in the biochemical analysis

of single-living cells and deliver gold nanoparticles by transient electroporation.

## 2 Materials and Methods

### 2.1 Preparation of Metallic Nanoparticles

Gold and silver nanoparticles were synthesized according to the protocols reported by Grabar et al.<sup>13</sup> and Munro et al.,<sup>14</sup> respectively. A Perkin–Elmer Lambda 950 spectrophotometer (Waltham, Massachusetts) and a Hitachi model H-800 transmission electron microscope (with an accelerating voltage of 200 kV) were used to characterize the prepared gold and silver nanoparticles.

### 2.2 Cell Culture

Human hepatoma carcinoma cells (HepG2 cell line) were obtained from the Fujian Provincial Cancer Hospital. The cells were grown as monolayers in Dulbecco’s modified eagle medium (DMEM) supplemented with 100 IU/mL penicillin/streptomycin and 10% fetal calf serum.

### 2.3 Cell Electroporation

Cell electroporation was carried out according to our previous studies.<sup>9,15</sup> In brief, cells were first harvested and resuspended in the medium with a density of  $1 \times 10^6$  cells/mL. Next, 400- $\mu$ L cell suspension and 100- $\mu$ L gold nanoparticles were mixed under 4°C in a 0.4-cm cuvette. After incubation for 10 min, the electroporation was processed using rectangular electric pulses with voltage of 375 V/cm, 1-ms duration time for two times utilizing a BTX-ECM 830 Electroporator (Bio-Rad Laboratories Ltd., Shanghai, China). Prior to Raman measurement, cells were washed exhaustively with phosphate buffer solution (PBS) by centrifuging at 1,000 rpm for 5 min to remove

\*Address all correspondence to: Juqiang Lin, E-mail: jqlin@fjnu.edu.cn; Rong Chen, E-mail: chenr@fjnu.edu.cn

<sup>†</sup>These authors have made equal contributions as cofirst authors.

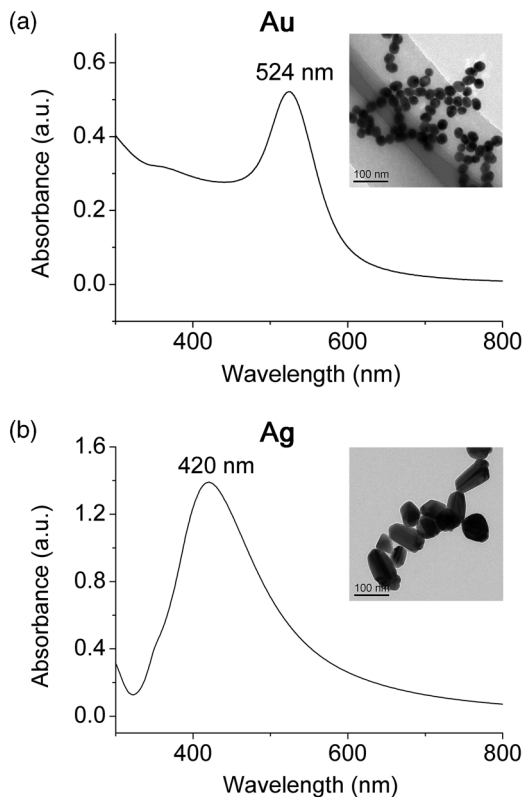


**Fig. 1** The UV-Vis absorption spectra of (a) gold nanoparticles (Au) and (b) silver nanoparticles (Ag) in water. The inserted figures show the transmission electron micrographs of gold nanoparticles and silver nanoparticles, respectively. Scale bars: 100 nm.

the nanoparticles, which were possibly attached to the cell exterior surface. The process was repeated several times. Ultimately, the living cells suspended in PBS were dropped and thinly spread on a stainless steel substrate, and the SERS measurements were performed immediately in order to maintain the activity of each cell.

#### 2.4 SERS Detection

A Renishaw Raman microscope (InVia system) and a 785-nm diode laser were used for the SERS measurement. Typically, the incident laser power was attenuated to 1 to 3 mW and the laser focus was enlarged up to 200% by adjustment of the pinhole

size. The enlarging the laser beam ( $\sim 20\text{-}\mu\text{m}$  size) was focused on the center of single-living cell (15 to  $20\text{-}\mu\text{m}$  size). In this case, the SERS spectrum of each living cell with good quality can be acquired by using a  $50\times$  objective. The fresh cells were redropped for each measurement in the range of  $560$  to  $1,730\text{ cm}^{-1}$  with a spectral resolution of  $2\text{ cm}^{-1}$ , each Raman spectra were acquired with a 10-s integration time.

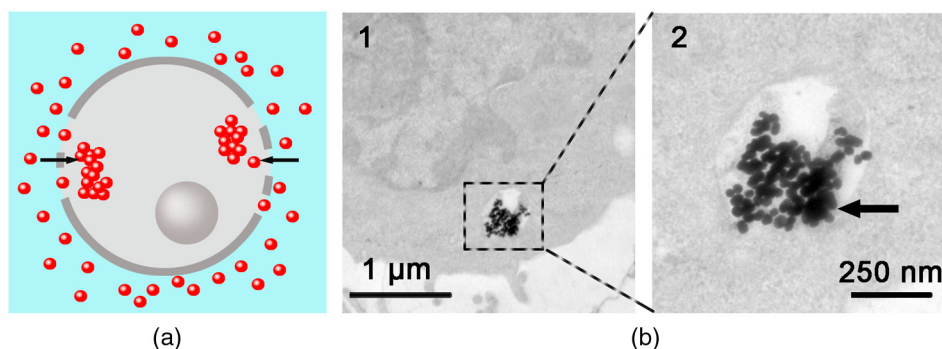
The software package of WIRE 2.0 (Renishaw) was employed for spectral acquisition and analysis. An automated algorithm, which was kindly offered by the BC Cancer Research Centre for autofluorescence background removal, was applied to the measured raw data to extract pure Raman spectra.<sup>16</sup> Then, each corrected SERS spectrum was normalized by the integrated area under the curve from  $560$  to  $1,730\text{ cm}^{-1}$ .

### 3 Results and Discussion

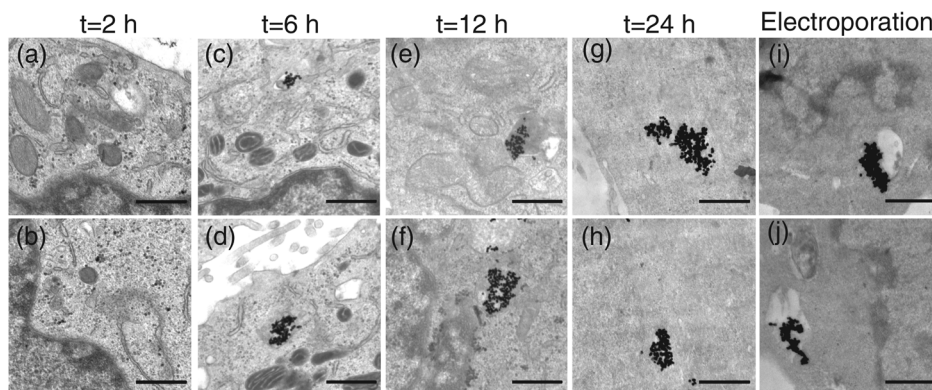
Figure 1(a) is the UV-Vis absorption spectrum of gold nanoparticles with an absorption peak at 524 nm. The transmission electron microscopy (TEM) photograph [inserted in Fig. 1(a)] of the gold nanoparticles shows the particle sizes follow a normal distribution with a mean diameter of 43 nm and standard deviation of 6 nm. The absorption peak of the silver nanoparticles is around 420 nm, and the TEM photograph reveals that the silver nanoparticles have a size distribution centered at about 60 nm in mean diameter [Fig. 1(b)].

Figure 2(a) shows the procedure for delivering gold nanoparticles into a cell by electroporation. Gold nanoparticles (red dots) are first mixed with cells in DMEM medium, and then there are a number of gold nanoparticles around the periphery of each of cells. The cell membrane acts as a barrier to the free diffusion of gold nanoparticles between the cytoplasm and the external medium. When the cells are treated by an electrical impulse, pores appear rapidly in the membrane, making cells highly permeable. During the effective pore open time, impermeable gold nanoparticles absorbed on or close to the membrane can freely diffuse through these openings into the cell interior. Once the electrical impulse fades, the membrane recovers its integrity and acts normally as the barrier again. Finally, gold nanoparticles are successfully trapped inside the cell.

Figure 2(b)-1 shows the TEM photograph of cell internalization of gold nanoparticles delivered by electroporation. Most of gold nanoaggregates locate in the cytoplasm; the magnification image [Fig. 2(b)-2] also indicates that the gold nanoparticles form a bigger nanoaggregate size in 300 nm or so, where the gaps between the spheroids can be vanishingly



**Fig. 2** (a) Schematic diagram of the procedure for delivering of gold nanoparticles (as indicated by red dots) into a cell by electroporation. (b) Transmission electron micrograph of gold nanoparticles in a HepG2 cell delivered by electroporation, and the rectangle area is the one with higher magnification. Scale bars: 250 nm.



**Fig. 3** (a)–(h) Parallel transmission electron micrographs of intracellular gold nanoparticles delivered by “passive uptake” (2, 6, 12, and 24-h incubation). (i) and (j) Parallel transmission electron micrographs of intracellular gold nanoparticles delivered by transient electroporation. Scale bars: 500 nm.

small in some area. There is a compelling evidence that these aggregated nanoparticles contain hot spots and can provide stronger SERS enhancement than individual particles.<sup>17–19</sup>

Figure 3 shows the parallel TEM photographs of the distribution of the intracellular gold nanoparticles, which were delivered by “passive uptake” (2, 6, 12, and 24-h incubation) and electroporation method, respectively. As shown in Figs. 3(a) and 3(b), gold nanoparticles could be observed over the entire cell after 2-h incubation, but mostly they are dimers and trimers. This indicates that it is hard for the clusters of nanoparticles to enter cells through “passive uptake.” At  $t = 6$  h [Figs. 3(c) and 3(d)], the clusters of gold nanoparticles begin to appear with irregular outlines. This aggregation inside cells is due to the interaction of the nanoparticles with components in the cellular environment.<sup>6</sup> With the increasing incubation times, the gold nanoaggregates significantly grow larger [Figs. 3(e)–3(h)], and the largest gold nanoaggregates are developed in lysosomes at 24 h in Figs. 3(g) and 3(h). In the electroporation experiment [Figs. 3(i) and 3(j)], the gold nanoaggregates can form as large as those developed through “passive uptake” by 24-h incubation in a very short time (within 1 min). Specially, the interparticle distance between gold nanoparticles delivered by electroporation method is closer than that transported by “passive uptake” (24-h incubation). In consideration of the distance dependence of plasmonic coupling, the closer interparticle distance in the assemblies of nanoparticles will achieve greater SERS signal enhancement;<sup>20,21</sup> therefore, gold nanoparticles aggregation developed by electroporation method may be more sensitive and effective in detecting intracellular components.

Figures 4(a) and 4(b) are the normalized mean SERS spectra of the individual HepG2 cells treated with silver nanoparticles and gold nanoparticles, respectively. The shaded areas represent the standard deviations of the means. In both figures, curve 1 is the cells subjected to the transient electroporation ( $n = 15$ ), and curve 2 is the cells incubated with nanoparticles for 24 h ( $n = 15$ ). Table 1 summarizes the tentative assignment of the observed SERS bands.<sup>2,22–31</sup> As shown in Fig. 4(a), the cells being treated with silver nanoparticles through electroporation (less than 1 min) and “passive uptake” experiment (24-h incubation) have significant differences in SERS spectral shapes, such as the appearance of 1,054 and 1,698- $\text{cm}^{-1}$  bands and a decrease in the intensity of 1,002 and 832- $\text{cm}^{-1}$  peaks for “passive uptake” [Fig. 4(a), curve 2]. Other peak positions include 662, 799, 1,340, and 1,416  $\text{cm}^{-1}$  for electroporation experiment shift to 668, 804, 1,344, and 1,397  $\text{cm}^{-1}$  for “passive uptake.” These spectral

changes may be related to the cellular toxicity caused by incubating with silver nanoparticles for a very long time (24 h). It has been demonstrated that the silver species release  $\text{Ag}^+$  ions and then interact with the thiol groups in proteins, affecting the replication of deoxyribonucleic acid.<sup>32,33</sup> However, the cells being delivered gold nanoparticles by these two methods have similar SERS spectral profiles [Fig. 4(b)], except for the band at 1,371  $\text{cm}^{-1}$ . The appearance of this peak is expected to be the result of higher signal enhancement, which is consistent with phenomena observed in Figs. 3(g)–3(j).

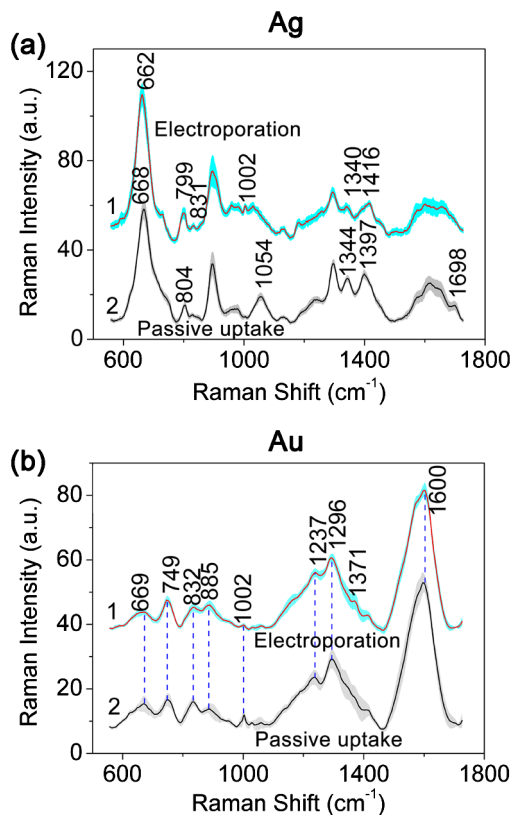


**Fig. 4** (a) Mean whole-cell surface-enhanced Raman scattering (SERS) spectra of the HepG2 cells ( $n = 15$ ) with silver nanoparticles (Ag) delivered by (1) transient electroporation and (2) “passive uptake” (24-h incubation). (b) Mean whole-cell SERS spectra of the HepG2 cells ( $n = 15$ ) with gold nanoparticles (Au) delivered by (1) transient electroporation and (2) “passive uptake” (24-h incubation).

**Table 1** Tentative assignment of the observed surface-enhanced Raman scattering (SERS) bands.

Raman shift (cm <sup>-1</sup> )	Tentative assignment <sup>a</sup>
662	$\nu$ (C–S)
669	T, G, $\nu$ (C–S)
749	T
799	Tyr, $\nu$ (C–S–C)
804	Tyr
832	Tyr
885	Tyr
1,002	Phe, p: $\nu$ (C–C)
1,054	$\nu$ (C–O), p: $\nu$ (C–N)
1,237	amide III
1,296	amide III
1,340	G, p: def (C–H)
1,344	p: def (C–H)
1,371	p: def (C–H)
1,416	aspartic and glutamic acids, $\nu$ (C–O)
1,600	Phe, Tyr

<sup>a</sup>p, protein;  $\nu$ , stretching; def, deformation; Tyr, tyrosine; Phe, phenylalanine; T, thymine; G, guanine.

## 4 Conclusion

To summarize, we have used the electroporation method for rapid delivery of gold nanoparticles into living HepG2 cells to achieve intracellular SERS spectra. Without decreasing the SERS enhancement, this method is much faster and more efficient than “passive uptake” in delivering gold nanoparticles into living cells. Furthermore, by comparison with silver nanoparticles, gold nanoparticles have better biological compatibility but less cellular toxicity. The results demonstrate that ultrasensitive gold nanoparticles—based SERS spectroscopy would allow to monitor very slight changes in chemical composition of living cells, which are very promising for developing a potential diagnosis method for cancer detection.

## Acknowledgments

This work was supported by the National Natural Science Foundation of China (Nos. 11274065, 61210016, 61178090, 61308113, 61178083, 81301253, and 61335011), Natural Science Foundation of Fujian Province (Nos. 2012J01254 and 2013J01225), the Science and Technology Project of Fujian Province (No. WKJ-FJ-01), and Program for Changjiang Scholars and Innovative Research Team in University (No. IRT1115). Peng Lu, Jing Wang, and Jinyong Lin designed the experiments, performed electroporation and Raman measurement, and wrote the paper together. Nenrong

Liu and Zufang Huang performed statistical analyses. Haishan Zeng and Buhong Li contributed to manuscript proof-reading. Juqiang Lin and Rong Chen managed the project. All authors participated in the discussion.

## References

1. K. Faulds et al., “Multiplexed detection of six labelled oligonucleotides using surface enhanced resonance Raman scattering (SERRS),” *Analyst* **133**(11), 1505–1512 (2008).
2. J. Kneipp et al., “Novel optical nanosensors for probing and imaging live cells,” *Nanomedicine* **6**(2), 214–226 (2010).
3. Y. Chen et al., “Label-free serum ribonucleic acid analysis for colorectal cancer detection by surface-enhanced Raman spectroscopy and multivariate analysis,” *J. Biomed. Opt.* **17**(6), 067003 (2012).
4. S. Xu et al., “Surface-enhanced Raman scattering studies on immunoassay,” *J. Biomed. Opt.* **10**(3), 031112 (2005).
5. A. Huefner et al., “Intracellular SERS nanoprobe for distinction of different neuronal cell types,” *Nano Lett.* **13**(6), 2463–2470 (2013).
6. J. Kneipp et al., “In vivo molecular probing of cellular compartments with gold nanoparticles and nanoaggregates,” *Nano Lett.* **6**(10), 2225–2231 (2006).
7. X. Tan et al., “Polyvinylpyrrolidone-(PVP-) coated silver aggregates for high performance surface-enhanced Raman scattering in living cells,” *Nanotechnology* **20**(44), 445102 (2009).
8. B. D. Chithrani, A. A. Ghazani, and W. C. Chan, “Determining the size and shape dependence of gold nanoparticle uptake into mammalian cells,” *Nano Lett.* **6**(4), 662–668 (2006).
9. J. Lin et al., “Rapid delivery of silver nanoparticles into living cells by electroporation for surface-enhanced Raman spectroscopy,” *Biosens. Bioelectron.* **25**(2), 388–394 (2009).
10. X. Huang and M. A. El-Sayed, “Gold nanoparticles: optical properties and implementations in cancer diagnosis and photothermal therapy,” *J. Adv. Res.* **1**(1), 13–28 (2010).
11. S. Feng et al., “Gold nanoparticle based surface-enhanced Raman scattering spectroscopy of cancerous and normal nasopharyngeal tissues under near-infrared laser excitation,” *Appl. Spectrosc.* **63**(10), 1089–1094 (2009).
12. K. Kneipp et al., “Surface-enhanced Raman spectroscopy in single living cells using gold nanoparticles,” *Appl. Spectrosc.* **56**(2), 150–154 (2002).
13. K. C. Grabar et al., “Preparation and characterization of Au colloid monolayers,” *Anal. Chem.* **67**(4), 735–743 (1995).
14. C. Munro et al., “Characterization of the surface of a citrate-reduced colloid optimized for use as a substrate for surface-enhanced resonance Raman scattering,” *Langmuir* **11**(10), 3712–3720 (1995).
15. J. Lin et al., “Electrical pulse-mediated enhanced delivery of silver nanoparticles into living suspension cells for surface enhanced Raman spectroscopy,” *Laser Phys. Lett.* **9**(3), 240 (2012).
16. J. Zhao et al., “Automated autofluorescence background subtraction algorithm for biomedical Raman spectroscopy,” *Appl. Spectrosc.* **61**(11), 1225–1232 (2007).
17. Y. Wang et al., “Surface enhanced Raman scattering of brilliant green on Ag nanoparticles and applications in living cells as optical probes,” *J. Phys. Chem. C* **111**(45), 16833–16839 (2007).
18. A. Otto et al., “Surface-enhanced Raman scattering,” *J. Phys.: Condens. Matter* **4**(5), 1143 (1992).
19. V. Joseph et al., “SERS enhancement of gold nanospheres of defined size,” *J. Raman Spectrosc.* **42**(9), 1736–1742 (2011).
20. Y. Wang, L. Tang, and J. Jiang, “Surface-enhanced Raman spectroscopy-based, homogeneous, multiplexed immunoassay with antibody-fragments-decorated gold nanoparticles,” *Anal. Chem.* **85**(19), 9213–9220 (2013).
21. K. Lee and J. Irudayaraj, “Correct spectral conversion between surface-enhanced Raman and plasmon resonance scattering from nanoparticle dimers for single-molecule detection,” *Small* **9**(7), 1106–1115 (2013).
22. J. Lin et al., “Investigation of free fatty acid associated recombinant membrane receptor protein expression in HEK293 cells using Raman spectroscopy, calcium imaging, and atomic force microscopy,” *Anal. Chem.* **85**(3), 1374–1381 (2013).

23. D. Serban, J. M. Benevides, and G. J. Thomas, "DNA secondary structure and Raman markers of supercoiling in Escherichia coli plasmid pUC19," *Biochemistry* **41**(3), 847–853 (2002).
24. I. Notingher et al., "Spectroscopic study of human lung epithelial cells (A549) in culture: living cells versus dead cells," *Biopolymers* **72**(4), 230–240 (2003).
25. R. Liu et al., "Surface-enhanced Raman scattering study of human serum on PVA—Ag nanofilm prepared by using electrostatic self-assembly," *J. Raman Spectrosc.* **42**(2), 137–144 (2011).
26. C. Xie et al., "Real-time Raman spectroscopy of optically trapped living cells and organelles," *Opt. Express* **12**(25), 6208–6214 (2004).
27. X. Yan et al., "Raman spectra of single cell from gastrointestinal cancer patients," *World J. Gastroenterol.* **11**(21), 3290 (2005).
28. J. W. Chan et al., "Micro-Raman spectroscopy detects individual neoplastic and normal hematopoietic cells," *Biophys. J.* **90**(2), 648–656 (2006).
29. M. Wang et al., "Optofluidic device for ultra-sensitive detection of proteins using surface-enhanced Raman spectroscopy," *Microfluid. Nanofluid.* **6**(3), 411–417 (2009).
30. M. Moreno et al., "Raman spectroscopy study of breast disease," *Theor. Chem. Acc.* **125**(3–6), 329–334 (2010).
31. G. P. Kumar et al., "Surface-enhanced Raman scattering studies of human transcriptional coactivator p300," *J. Phys. Chem. B* **110**(33), 16787 (2006).
32. G. Martinez-Castanon et al., "Synthesis and antibacterial activity of silver nanoparticles with different sizes," *J. Nanopart. Res.* **10**(8), 1343–1348 (2008).
33. M. Marini et al., "Antibacterial activity of plastics coated with silver-doped organic-inorganic hybrid coatings prepared by sol-gel processes," *Biomacromolecules* **8**(4), 1246–1254 (2007).

**Peng Lu** is currently researching the optical detection of cancer cells by surface-enhanced Raman spectroscopy for his master's degree under the supervision of Rong Chen and Juqiang Lin.

**Jing Wang** is currently studying for her master's degree under the supervision of Rong Chen and Juqiang Lin. She is currently researching the application of SERS for biomedical study.

**Jinyong Lin** is currently researching the label-free detection of type 2 diabetes by Raman spectroscopy for his master's degree under the supervision of Rong Chen and Juqiang Lin.

**Juqiang Lin** received his PhD degree of biomedical engineering in Huazhong University of Science and Technology in 2006. Then, he went to Utah State University as a visiting scholar (2009 to 2011). His research interests include Raman spectroscopy and biomedical photonics imaging.

**Nenrong Liu** received her PhD degree in optical engineering from Fujian Normal University in 2014. Her technical research is mainly about nonlinear spectroscopy and biomedical imaging for noninvasively early cancer diagnosis.

**Zufang Huang** obtained his PhD degree in 2013 from Fujian Normal University in medical spectroscopy and spectral analysis. He is now mainly focusing on the diagnosis and quantitative analysis of human fluids by using Raman spectroscopy and SERS.

**Buhong Li** is a professor and vice dean with the School of Photonics and Electronic Engineering at Fujian Normal University. He earned his PhD degree in optical engineering from Zhejiang University in 2003. His research interests include fluorescence and Raman spectroscopy, and the mechanism and dosimetry for photodynamic therapy.

**Haishan Zeng** is a distinguished scientist with the Integrative Oncology Department (Imaging Unit) of British Columbia Cancer Agency Research Centre, Vancouver, Canada, and an associate professor of dermatology and skin science at the University of British Columbia (UBC). For over 20 years, his research has been focused on developing various optical imaging and spectroscopy techniques for improving early cancer detection.

**Rong Chen** is a professor of the School of Optoelectronics and Information Engineering, Fujian Normal University, China. His research interest focuses on the application of Raman spectroscopy in biomedical detection.